# Capacitive Sensing for a Gripper with Gecko-Inspired Adhesive Film

Jiro Hashizume[1], Tae Myung Huh[2], Srinivasan A. Suresh[2], and Mark R. Cutkosky[2]

***Abstract*—We present a capacitive sensor suitable for a gripper that uses thin films of gecko-inspired adhesives. The sensor is fabricated directly on the films and measures the area over which the adhesive makes intimate contact. In experiments, a new under-actuated gripper uses adhesive films to acquire and hold objects having a variety of shapes and textures. Using the adhesive films, the gripper achieves 2.6x greater pullout force on rough surfaces as compared to using soft rubber. For a good grip, as the applied load increases, the films adhere more tightly to object surfaces and the local capacitance increases at contact regions. With six taxels per finger, the sensor can also detect whether the contact pattern of a grasp matches expectations.**

***Index Terms*—Perception for Grasping and Manipulation, Force and Tactile Sensing, Soft Sensors and Actuators, Grippers and Other End-Effectors**

## I. Introduction

In autonomous robotic manipulation, the ability to grasp objects of widely varying shapes and sizes is an important challenge and has lead to many efforts to equip mobile robots with hands that are more versatile than industrial grippers. Dexterous hands represent one solution, but they are typically heavy, delicate, expensive and complex to control. A popular alternative is to use compliant under-actuated hands. Recent hand reviews include [1]–[3] and analysis methods for under-actuated hands are presented in [4], [5]. However underactuated hand design incurs tradeoffs. If the gripper will lift heavy objects and hold them securely it typically needs to be capable of large grasp forces, which again increases weight and cost. Conversely if the gripper relies on conforming closely to a wide range of shapes using a soft structure it often lacks precision, especially when working with tools. The compliant gripper presented here (Fig. 1) provides a combination of ability to partially wrap around objects and to hold small parts securely in a fingertip pinch.

A useful approach to increase the capability of compliant hands is to augment them with an astrictive technology [6] for example suction, magnetic, electrostatic or van der Waals forces, all of which can greatly increase the available load force for a given grasp force. In particular, gecko-inspired adhesives using van der Waals forces have been demonstrated on industrial grippers [7], soft pneumatic fingers [8] and in a minimalist thin-film gripper that can grasp objects without squeezing [9]. The same shear-activated adhesive technology is used here. Other examples of adhesive or hybrid electrostatic/adhesive gripping include [10]–[14].

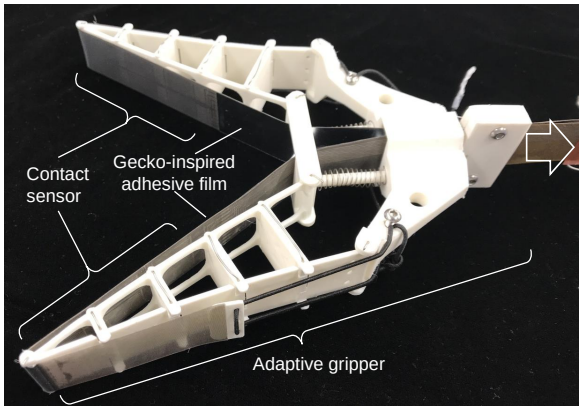


Fig. 1: Adaptive soft exoskeleton gripper with the directional adhesive gecko films equipped with the contact sensor.

However, a less explored issue for such grippers is to sense the state of adhesive contacts. For an adhesion-based gripper, this information is crucial to prevent grasp failures. It does not suffice to monitor the grasp force because adhesion depends mainly on the intimate area of contact with an object surface and not on the normal force. Thus we desire a sensor that will reliably determine the area of contact when a compliant adhesive gripper attempts to grasp an object. Ideally the sensor should also provide a warning of impending grasp failure. One approach used for adhesives mounted on rigid tiles is to measure the normal and shear stresses at 4 taxels and monitor their ratio to detect incipient failure [15]. This approach will not work for thin films. However, an approach using polyvinylidene fluoride (PVDF) transmitters and receivers has been shown to indicate the level of adhesion on a film of gecko-inspired adhesive contacting a substrate [16].

Here we present an alternative approach that is particularly suitable for an underactuated gripper that exploits gecko-inspired adhesives. The sensor is fabricated in-situ with thin adhesive films on each finger and measures the change in capacitance that occurs when a region of adhesive makes contact with a surface. The local capacitance increases as the adhesive adheres more strongly in response to an applied shear load.

In the following sections, we first describe the design of the new adaptive soft gripper and the capacitive sensor incorporated into its adhesive fingers. We then present results

Manuscript received: September, 10, 2018; Revised November, 8, 2018; Accepted January, 2, 2019.

This paper was recommended for publication by Editor Han Ding upon evaluation of the Associate Editor and Reviewers' comments.

[1]J. Hashizume is with Hitachi America Ltd, 3315 Scott Blvd, 4th Floor, Santa Clara, CA 95054, USA j.hashizume55@gmail.com

[2]T. M. Huh, S. A. Suresh and M. R. Cutkosky are with The Center for Design Research, Stanford University, Stanford, CA 94305, USA

Digital Object Identifier (DOI): see top of this page.

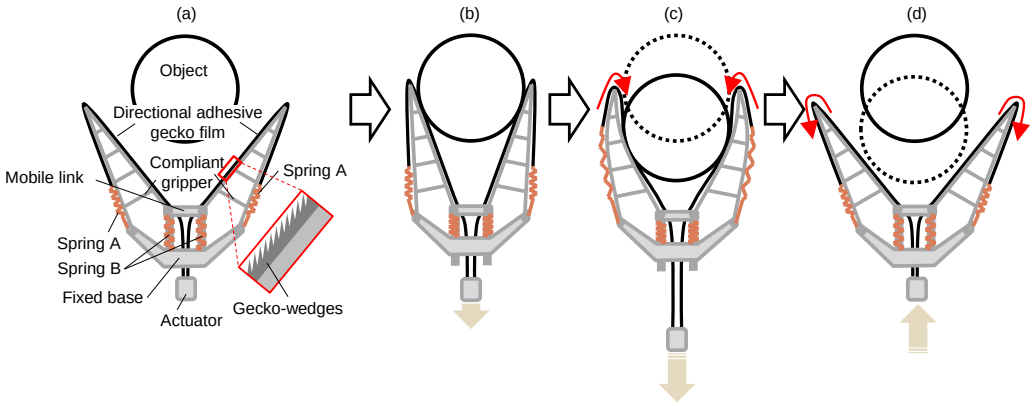


Fig. 2: (a) Initial configuration of our adaptive soft exoskeleton gripper. Gecko-inspired adhesive film is wrapped around the gripper finger and the trailing end is connected via spring A to the fixed base. The adhesive is oriented to apply shear towards the fixed base of the gripper, allowing it to acquire and retain the target object. (b) The gripper fingers close and contact the object when a tension force is applied to the actuator. (c) As the tension increases, the object is retracted and wrapped by the directional adhesive gecko film. (d) Releasing the tension force releases the object.

of grasping and sensing experiments, showing that the sensor can detect when the adhesive films make contact and that they provide a measure of the contact area.

## II. Design and Fabrication

### A. Adaptive Gripper

The compliant gripper depicted in Figs. 1 and 2 has two fingers covered with adhesive films. A single actuator pulls on the films, which pass through the palm. The fingers are inspired by the Festo FinGripper [17], but are composed of plastic links connected with pin joints. Hence they are relatively stiff when used for a fingertip pinch.

Figure 2 (b-d) shows the actuating sequence. The adhesive films are attached at their trailing ends to springs, A. As the actuator pulls on the inner (proximal) ends of the films, the films slide slightly on the fingers and stretch the springs A, which have a stiffness of approximately $32\,\mathrm{mN/mm}$. The films also exert forces at the tips of the fingers, which tend to close the fingers. A pair of soft springs in the palm, B, ($76\,\mathrm{mN/mm}$) provide a restoring force to keep the films taut and open the fingers. The overall function of the mechanism is that as the fingers close, there is also an inward pulling motion on the films, which tends to draw objects into the grasp as seen in Fig. 2 (c). A related concept has been demonstrated in non-adhesive grippers [18].

As illustrated in Fig. 2 (a), the surfaces of the films are covered with microscopic silicone rubber wedges (Sylgard 170, Dow Corning) with a triangular profile, approximately $40\,\mu\mathrm{m}$ wide at the base and $100\,\mu\mathrm{m}$ long. As the films make contact with an object, loading them in shear causes the wedges to bend flat, which produces adhesion. The typical stress for gripping a smooth surface is approximately $60\,\mathrm{kPa}$ when loaded in shear [9], and increases with increasing normal pressure. The design and fabrication process for creating films with these wedges is covered in detail in [19], [20]. The backing is $25\,\mu\mathrm{m}$ film, which can be either polyimide or Mylar polyester with a metalized surface for the sensor described in the next section.

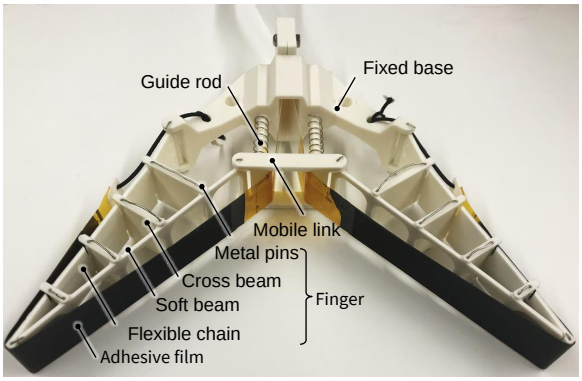


Fig. 3: Each finger skeleton consists of a *flexible chain* of segments connected by pins to *cross beam* struts and a compliant inner *soft beam* that bends to conform to curved surfaces. These are mounted to a *fixed base* and moved by a moving *mobile link*. All parts are printed from ABS plastic.

The plastic gripper components illustrated in Fig. 3 are all 3D printed from ABS plastic (Ultimaker 3 Extended). The flexible chain on the outer side of each finger provides no bending stiffness; the soft beam on the inner side has large cutouts to give it low bending stiffness so that the fingers can conform to curved objects (visible in some of the grasping experiments shown later in Fig. 10).

### B. Contact Sensor

To measure object contact while grasping, we designed a capacitive sensor using six taxels with interdigital electrodes, fabricated directly in the adhesive films, as seen in Fig. 4 (top). The lower part of Fig. 4 illustrates how capacitance increases as the wedges make initial contact (b) and finally become fully compressed (c) when a shear load is applied. The change in capacitance results both from a decrease in the object distance and an increase in the effective dielectric constant for silicone rubber versus air. The 6 taxels have an area of $15 \times 7\,\mathrm{mm}$ each, and allow us to measure the spatial distribution of the contact.

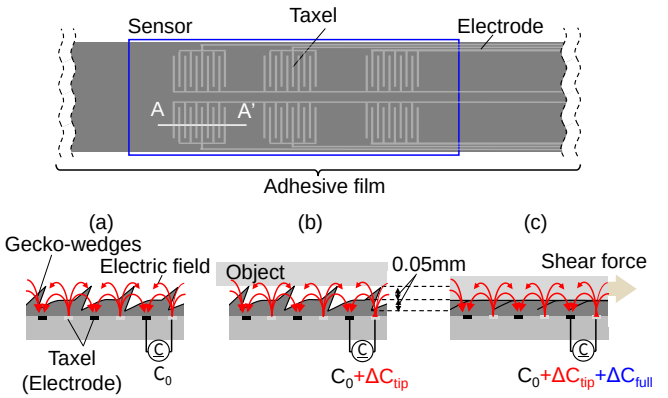


Fig. 4: *Top*: Sensing pattern, showing interdigitated electrodes in each taxel and arrangement of taxels. *Bottom*: Taxels have initial capacitance of $C_0$ prior to contact (a). When the wedge tips make contact, the object interacts with the taxels to increase capacitance by $\Delta C_{\text{tip}}$ (b); when loaded, the wedges form a nearly continuous surface and elimination of the air gap further increases capacitance by $\Delta C_{\text{full}}$ (c).

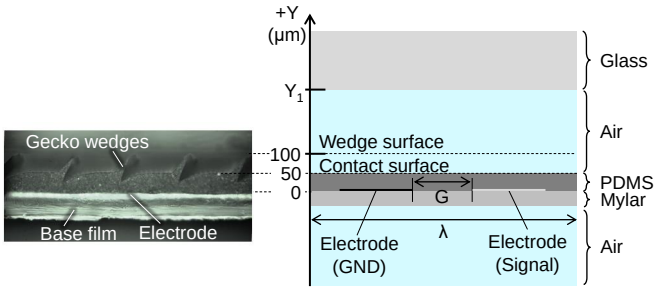


Fig. 5: *Left*: Cross-sectional image of the fabricated adhesive film. *Right*: 2D simulation model to evaluate the electrode design.

To explore appropriate dimensions for the electrode patterns, We used finite element analysis (FEA) software (COMSOL Multiphysics) with a simplified 2D model; we assumed that the interdigital electrode gaps and sensor/object distance are sufficiently small compared to overall taxel size that a 3D analysis is not required to explore effects of changes in parameters. From a microscopic side view of the adhesive wedges, we built a 2D model that assumes periodic patterns of interdigital electrodes (Fig. 5). We simplify the wedge geometry to a stack of a solid layer of polydimethylsiloxane (PDMS) ($50\,\mu\text{m}$) and an air layer ($50\,\mu\text{m}$), assuming low fill ratio around the tips of the wedges. The detailed parameters are given in Table I. In simulation, we varied the spatial wavelength of interdigital electrodes, $\lambda$, and the gap between the ground and the signal electrode, $G$, which are significant variables in prior studies [21], [22].

Using simulations, we explored electrode dimensions that would provide high sensitivity to changes in contact without extending the field so far that the taxel becomes a proximity sensor. Fig. 6 shows the simulated capacitance change of taxels as they go from tip contact to full contact ($\Delta C_{\text{full}}$ in Fig. 4), as a function of $\lambda$ and $G$. For $25\,\mu\text{m} \leq G \leq 400\,\mu\text{m}$, we found the maximum $\Delta C_{\text{full}}$ at $\lambda = 1 \sim 1.5\,\text{mm}$. For $\lambda <$

TABLE I: Simulation Parameters

| **Physical Parameters** | $\epsilon_r$ | Thickness, μm |
|---|---|---|
| Base film (Mylar) | 3.25 | 25 |
| Wedges (PDMS) | 2.75 | 50 |
| Object (glass) | 7.50 | 1000 |
| **Contact Conditions** | | $Y_1$, μm |
| No Contact | | $\infty$ |
| Tip Contact | | 100 |
| Full Contact | | 50 |

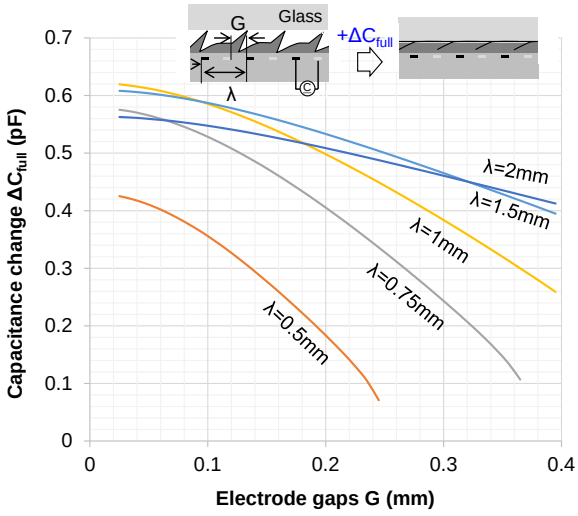


Fig. 6: Simulated capacitance change of the contact taxel in the adhesive film for different electrode patterns. Capacitances are computed for a sensing area of $15\,\text{mm} \times 7\,\text{mm}$.

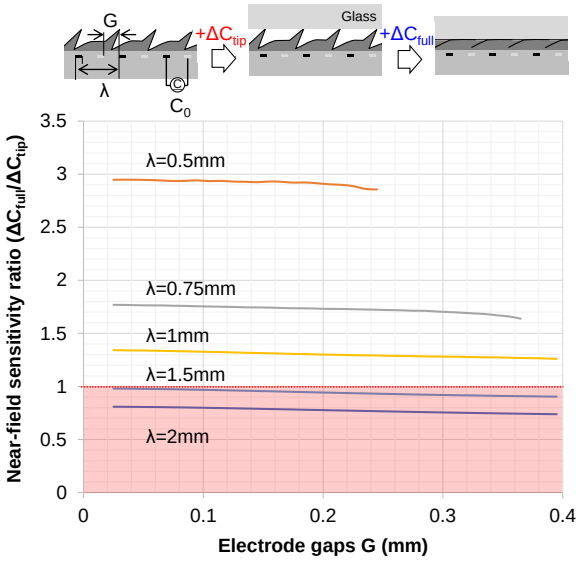


Fig. 7: Simulated near-field sensitivity ratio ($\Delta C_{\text{full}}/\Delta C_{\text{tip}}$) dependence on the spatial wavelength $\lambda$ and gap distance $G$.

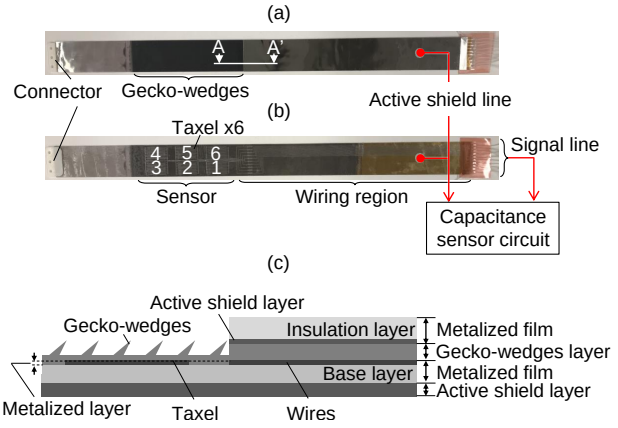


Fig. 8: (a) Front (contact) side of the adhesive film. Black regions represent the gecko-wedges area. Electrodes to connect to the capacitance sensor are at the right edge of the film. (b) Back side of the adhesive film. The sensing region is composed of six independent contact taxels. (c) Cross-sectional image (A-A') of the adhesive film.

$1\,\mathrm{mm}$, the electric fields do not expand enough to detect the contact changes within the wedge heights. For $\lambda > 1.5\,\mathrm{mm}$, the electric fields expand much farther than wedge heights, and thus contact changes do not contribute strongly to $\Delta C_{\text{full}}$. For fixed $\lambda$, $\Delta C_{\text{full}}$ increases with smaller $G$ due to stronger fringe effects. However, the smallest length of $G$ will be limited by the fabrication constraints.

To ensure robust detection of contact rather than simply proximity, we want each taxel to respond more strongly to changes in contact ($\Delta C_{\text{full}}$) than to changes in proximity ($\Delta C_{\text{tip}}$); we define the near-field sensitivity ratio as the ratio of these responses, $\Delta C_{\text{full}}/\Delta C_{\text{tip}}$. Fig. 7 shows that the near-field sensitivity ratio decreases as $\lambda$ increases while $G$ does not cause noticeable changes. If the ratio is one or lower, the taxel becomes too sensitive to objects which are close but not in contact. Based on the results of the analysis and given manufacturing constraints on minimum feature size, we chose $\lambda = 1\,\mathrm{mm}$ with $G = 0.25\,\mathrm{mm}$.

The contact sensors are fabricated directly on the metalized backing for the adhesive film strips. The front (contacting) face of the film is shown in Fig. 8 (a). On the back side of the film (Fig. 8 (b)) the 6 taxels are patterned in the metalized layer (Al, $40\,\mathrm{nm}$). Fig. 8 (c) illustrates a cross section of the film.

The electrode pattern is directly ablated into the metalized film using a UV laser with $\approx 8\,\mu\mathrm{m}$ spot size, at a low enough power to avoid cutting the base layer. The wedges are cast directly atop this pattern. Traces connecting the electrodes to the end of the film were also directly patterned in the metalized layer. The non-sensing region is covered with a second metalized film that provides an active shield, which increases the signal/noise ratio. Above the active shield there is a thin insulation layer.

On the back, non-contacting, side of the film there is a second active shield of thin metal fabric glued in place using flexible adhesive (Sil-Poxy, Smooth-On). The active shield layers and the signal lines are connected to the active shield terminal and signal terminal respectively of a capacitance-to-digital circuit (AD7147, Analog Devices, sampling at 108Hz), respectively.

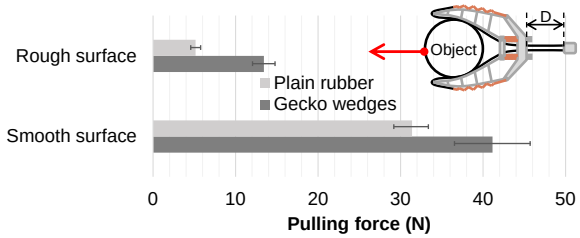


Fig. 9: Pullout force of the gripper under various grasp conditions. Pullout forces on the smooth cylinder are consistently higher than on the rough. In both cases, using adhesive films on the gripper yields a significant improvement.

## III. Experiments

### A. Grasping Experiments

We conducted a series of tests to measure quantitative effects of the gecko adhesives on pullout force, as well as several tests to demonstrate the versatility and robustness of the gripper on a variety of objects.

First, we evaluated the effect of gecko adhesives in increasing pullout force by performing tests on cylinders. The cylinders are $63\,\mathrm{mm}$ in diameter with two different surface conditions: the first with a smooth acrylic surface and the other covered by masking tape (#2090, 3M), resulting in a textured surface. We used two gripper configurations: one with gecko wedges on the films and the other with a plain PDMS layer on the films. For each test, we placed the object at a fixed position with respect to the gripper, and loaded the film of the gripper to a fixed tension of $9.8\,\mathrm{N}$. After the initial grip, we locked the film with respect to the gripper base, keeping the distance $D$ between the actuator and the fixed base constant (Fig. 9). We then applied a force pulling the object out of the grasp and measured the force magnitude when the contact first slipped. Each test was repeated several times.

Fig. 9 shows the maximum pullout forces on the two cylinders using smooth PDMS and adhesive films in the gripper. Pullout forces are significantly higher on the smooth surface than on the rough surface for both types of films. On the smooth cylinder, the adhesive films have a pullout force 1.3 times larger than that using smooth PDMS ($41.1\,\mathrm{N}$ and $31.4\,\mathrm{N}$, respectively). On the rough surface, although the magnitudes of the forces are lower, the adhesive films achieve pullout forces 2.6 times larger than those achieved by plain PDMS ($13.4\,\mathrm{N}$ and $5.2\,\mathrm{N}$, respectively).

We evaluated the versatility of the gripper by testing it on several objects of varying size, shape, texture, weight and softness, as seen in Fig. 10. For each object, we followed the same procedure as on the cylinders to initially grasp the object, first tensioning the films to $9.8\,\mathrm{N}$ and then fixing them in place. In each case the gripper was able to partially conform to the object and lift it. On smooth objects (a, c, d, g), the adhesive substantially increases the lifting force, even when the object has a non-uniform shape (d), or deforms (g). In the case of large, smooth objects (a) the gripper grasps and lifts objects

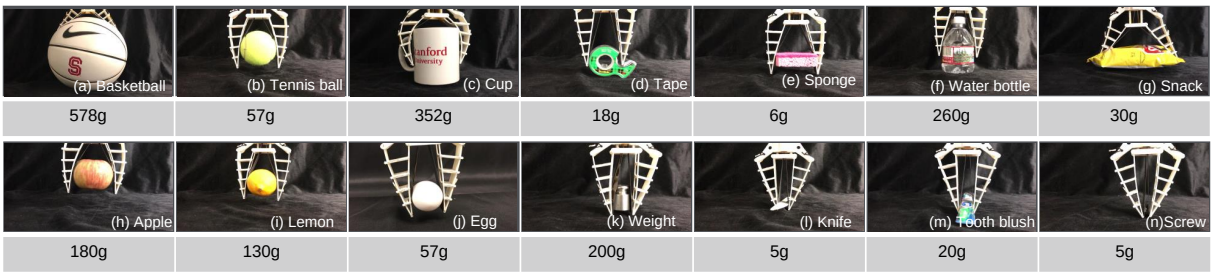


Fig. 10: Grasping examples with our adaptive soft exoskeleton gripper.

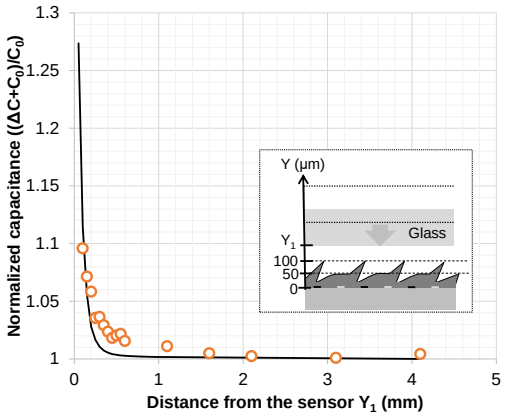


Fig. 11: Normalized capacitance of sensor versus distance between the sensor and a glass plate. Black line and Orange circles show the simulation and measurement results, respectively.

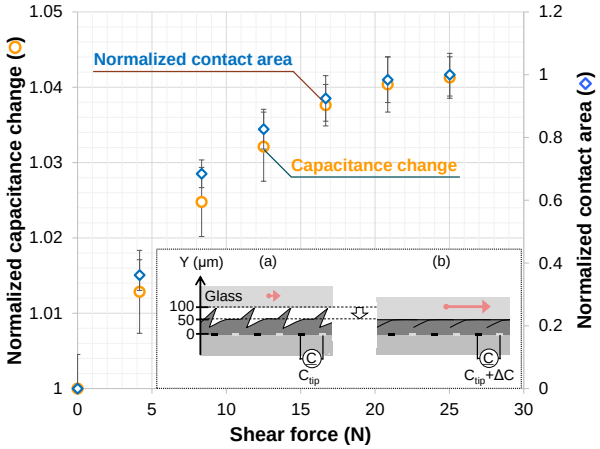


Fig. 12: Normalized capacitance change $(C_0 + \Delta C)/C_{\text{tip}}$ and contact area (right vertical axis) as shear stress is applied: (a) initial contact, (b) wedges fully flattened.

using the gecko adhesive film where either no grasp or only marginal grasps are possible with smooth PDMS films.

Although objects with rough surfaces (b), sparse surface structures (e), or low contact areas (l, m, n) do not allow substantial adhesion, these objects are still successfully grasped using a combination of adhesive film retraction (as the actuator pulls) and conformation of the fingers.

### *B. Sensor Evaluations*

We evaluated the contact sensor with a single taxel sample of the gecko-inspired adhesive film. For better signal to noise ratio during evaluation, we amplified sensor responses by making the test taxel larger ($33 \times 24\,\text{mm}$) while keeping other parameters the same as in Section II-B ($\lambda = 1\,\text{mm}$, $G = 0.25\,\text{mm}$). We placed a glass plate ($75\times\ 55\times\ 1\,\text{mm}$) on the film and controlled the gap by using different spacers between the glass plate and the sensor.

Fig. 11 shows the normalized capacitance $(C_0 + \Delta C)/C_0$ as a function of object distance from the sensor. Here, $\Delta C$ is the capacitance change from the initial capacitance $C_0$. The black line is the normalized capacitance calculated from the FEA, with measured values plotted as orange circles. The capacitance is much more sensitive at smaller gaps as the electric field is strongly localized near the interdigital electrodes.

Using the same test sample, we compared the change in capacitance and real contact area as we applied a shear load to the adhesive, flattening the wedges and increasing contact

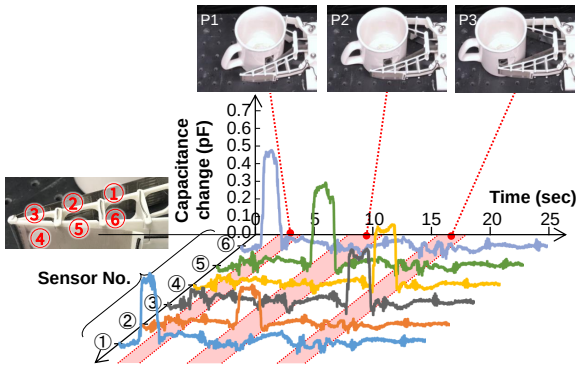


Fig. 13: *Top*: figures show the experimental setup and grasping condition in each cup position (P1, P2, P3). *Bottom*: figure shows each contact signal coming from the 6 contact taxels during the gentle grasps.

(starting at $Y = 100\,\mu\text{m}$ and $0\,\text{kPa}$ shear stress). The real contact area was measured by using frustrated total internal reflection (FTIR), as used in previous works [7], [15] to measure where the adhesive makes intimate contact with the adherend surface. As the two curves in Fig. 12 show, the change in capacitance and the real area of contact track each other closely, and both correspond to an increase in the applied shear force.

### *C. Sensor-based Grasping Experiments*

Using the gripper with gecko adhesive films and contact sensors, we tested the ability to detect initial contact locations

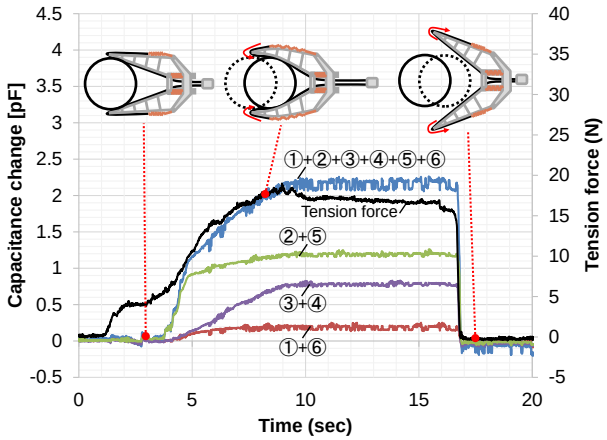


Fig. 14: Capacitance changes at taxels while grasping a ceramic mug.

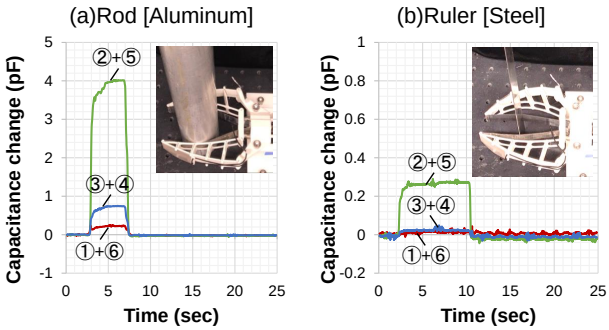


Fig. 15: Capacitance changes while grasping rounded (left) and sharp-edged (right) metal objects.

and measure contact area during grasping. In this case we considered only symmetric grasps, and instrumented only one finger of the gripper, with the numbering of the taxels shown in the left inset of Fig. 13.

For contact location tests, we placed an object (a cup) at three different positions, called P1, P2, and P3 as shown in Fig. 13 (top). Each of these locations corresponds to different sensing areas: P1, contacting taxels ① and ⑥, which are located proximally; P2, at taxels ② and ⑤, in the center of the finger; P3, at taxels ③ and ④, located distally. For each position, we applied tension to the actuator such that the gripper gently contacted the object without saturating the sensors.

The measured data are plotted in Fig. 13 (bottom), and show that during each contact (red shaded periods) only the corresponding taxels respond, without significant crosstalk. The sensor can therefore detect the initial contact locations of the gripper, which could be valuable for robust grasp planning and control [23], [24].

To monitor changes of contact area during a grasp, we evaluated the sensor outputs as the grasp went from the gentle initial contacts to a firm grip. We placed the object at P2, and increased the tension of the adhesive films, which draws the object into the grasp and conforms the fingers to the object in a firm grasp.

Figure 14 shows the capacitance change of each segment during this process. As in Fig. 13, the initial contact is made on the middle taxels (②, ⑤) which respond quickly to the intital contact. As tension increases further, the capacitance of the other taxels increases, without compromising the initial contact. This result indicates that as the gripper applies more grasping force, the gripper conforms to the object and adds contact area, providing more adhesion.

When grasping a thin object or an object with sharp corners, the contact may occupy only a small portion of a single taxel. In this case, as seen in Fig. 15, the change in capacitance is considerably less than for a gently rounded object but remains detectable. A limiting case would be where a line contact occurs at the border between two taxels and could be missed. This is a known problem in tactile sensing and can be addressed by increasing the thickness of an elastic skin above the tactile sensors, which spreads the impulsive pressure distribution [25], [26]. However, in this design it would also reduce the ability of the thin film to conform to irregular surfaces. Comparing Figs. 14 and 15 also shows that while the change in initial capacitance is considerably larger for metallic versus ceramic objects, the onset of contact and the subsequent trend of increasing capacitance with increasing shear load are clearly visible in both cases. If it is desired to obtain a more uniform response for a variety of materials a couple of options are possible. The first is to normalize the change in capacitance by the magnitude of the initial jump in capacitance as the object first makes contact. The second is to provide an additional calibration taxel, with no wedges (and therefore no change in capacitance on loading) and to use the value from that taxel to normalize the readings from the other taxels.

## IV. Conclusion

In this study, we have presented an adaptive compliant, underactuated gripper equipped with a flexible contact sensor. The gripper exploits directional gecko-inspired adhesives to increase the maximum force that it can sustain at light grasping forces. The adhesives are mounted to thin films and actuated to load the films with a shear force that engages the adhesive and tends to draw an object into the gripper as the fingers close. In experiments the gripper was able to grip a range of common objects with light tension forces of $\approx 9.8\,\mathrm{N}$, in part due to the use of adhesives and in part due to the ability of the fingers to adapt to object curvature.

Laser patterning of a thin metal layer creates an interdigital capacitive sensor on the flexible films, with six taxels for each finger. Tests on the sensor showed that the capacitance increases locally at each taxel as an area of film first makes contact, and then continues to increase with increasing shear load at the contact. In a successful grasping operation one can observe the sequence of capacitance increases along the taxels as an object first contacts the fingertips and then is drawn toward the palm.

As future steps we plan to monitor the sensors for indications of incipient grasp failure when loads increase unexpectedly. Another interesting extension is to implement a referencing sensor that measures material properties, which would allow calibration per material to obtain the real contact area.

## V. Acknowledgments

T.M. Huh is partially supported by a Samsung Scholarship and by NSF NRI 1528145. S.A. Suresh is supported by a NASA Space Technology Research Fellowship. M.R. Cutkosky is partially supported by NASA ESI grant NNX16AD19G.

## References

[1] J. T. Belter and A. M. Dollar, "Performance characteristics of anthropomorphic prosthetic hands," in *Rehabilitation Robotics (ICORR), 2011 IEEE International Conference on*. IEEE, 2011, pp. 1–7.

[2] M. Controzzi, C. Cipriani, and M. C. Carrozza, "Design of artificial hands: A review," in *The Human Hand as an Inspiration for Robot Hand Development*. Springer, 2014, pp. 219–246.

[3] C. Melchiorri and M. Kaneko, "Robot hands," in *Springer Handbook of Robotics*. Springer, 2016, pp. 463–480.

[4] L. Birglen, T. Laliberté, and C. M. Gosselin, *Underactuated Robotic Hands*, ser. Springer Tracts in Advanced Robotics. Springer, 2007, vol. 40.

[5] G. A. Kragten and J. L. Herder, "The ability of underactuated hands to grasp and hold objects," *Mechanism and Machine Theory*, vol. 45, no. 3, pp. 408–425, 2010.

[6] G. J. Monkman, "An analysis of astrictive prehension," *The International Journal of Robotics Research*, vol. 16, no. 1, pp. 1–10, 1997.

[7] J.-P. Roberge, W. Ruotolo, V. Duchaine, and M. Cutkosky, "Improving industrial grippers with adhesion-controlled friction," *IEEE Robotics and Automation Letters*, vol. 3, no. 2, pp. 1041–1048, 2018.

[8] P. Glick, S. A. Suresh, D. Ruffatto, M. Cutkosky, M. T. Tolley, and A. Parness, "A soft robotic gripper with gecko-inspired adhesive," *IEEE Robotics and Automation Letters*, vol. 3, no. 2, pp. 903–910, 2018.

[9] E. W. Hawkes, H. Jiang, D. L. Christensen, A. K. Han, and M. R. Cutkosky, "Grasping without squeezing: Design and modeling of shear-activated grippers," *IEEE Transactions on Robotics*, vol. 34, no. 2, pp. 303–316, 2018.

[10] M. Dadkhah, Z. Zhao, N. Wettels, and M. Spenko, "A self-aligning gripper using an electrostatic/gecko-like adhesive," in *Intelligent Robots and Systems (IROS), 2016 IEEE/RSJ International Conference on*. IEEE, 2016, pp. 1006–1011.

[11] J. Shintake, S. Rosset, B. Schubert, D. Floreano, and H. Shea, "Versatile soft grippers with intrinsic electroadhesion based on multifunctional polymer actuators," *Advanced Materials*, vol. 28, no. 2, pp. 231–238, 2016.

[12] H. Jiang, E. W. Hawkes, C. Fuller, M. A. Estrada, S. A. Suresh, N. Abcouwer, A. K. Han, S. Wang, C. J. Ploch, A. Parness *et al.*, "A robotic device using gecko-inspired adhesives can grasp and manipulate large objects in microgravity," *Sci. Robot*, vol. 2, no. 7, 2017.

[13] S. Song, D.-M. Drotlef, C. Majidi, and M. Sitti, "Controllable load sharing for soft adhesive interfaces on three-dimensional surfaces," *Proceedings of the National Academy of Sciences*, vol. 114, no. 22, pp. E4344–E4353, 2017.

[14] J. Guo, K. Elgeneidy, C. Xiang, N. Lohse, L. Justham, and J. Rossiter, "Soft pneumatic grippers embedded with stretchable electroadhesion," *Smart Materials and Structures*, vol. 27, no. 5, p. 055006, 2018.

[15] X. A. Wu, D. L. Christensen, S. A. Suresh, H. Jiang, W. R. Roderick, and M. Cutkosky, "Incipient slip detection and recovery for controllable gecko-inspired adhesion," *IEEE Robotics and Automation Letters*, vol. 2, no. 2, pp. 460–467, 2017.

[16] T. M. Huh, C. Liu, J. Hashizume, T. G. Chen, S. A. Suresh, F.-K. Chang, and M. R. Cutkosky, "Active sensing for measuring contact of thin film gecko-inspired adhesives," *IEEE Robotics and Automation Letters*, vol. 3, no. 4, pp. 3263–3270, 2018.

[17] M. Wilson, "Festo drives automation forwards," *Assembly Automation*, vol. 31, no. 1, pp. 12–16, 2011.

[18] V. Tincani, G. Grioli, M. G. Catalano, M. Garabini, S. Grechi, G. Fantoni, and A. Bicchi, "Implementation and control of the velvet fingers: A dexterous gripper with active surfaces," in *2013 IEEE International Conference on Robotics and Automation*, May 2013, pp. 2744–2750.

[19] P. Day, E. V. Eason, N. Esparza, D. Christensen, and M. Cutkosky, "Microwedge machining for the manufacture of directional dry adhesives," *Journal of Micro and Nano-Manufacturing*, vol. 1, no. 1, p. 011001, 2013.

[20] S. A. Suresh, D. L. Christensen, E. W. Hawkes, and M. Cutkosky, "Surface and shape deposition manufacturing for the fabrication of a curved surface gripper," *Journal of Mechanisms and Robotics*, vol. 7, no. 2, p. 021005, 2015.

[21] Y. Huang, Z. Zhan, and N. Bowler, "Optimization of the coplanar interdigital capacitive sensor," in *AIP Conference Proceedings*, vol. 1806, no. 1. AIP Publishing, 2017, p. 110017.

[22] R. Igreja and C. Dias, "Analytical evaluation of the interdigital electrodes capacitance for a multi-layered structure," *Sensors and Actuators A: Physical*, vol. 112, no. 2-3, pp. 291–301, 2004.

[23] R. Calandra, A. Owens, D. Jayaraman, J. Lin, W. Yuan, J. Malik, E. H. Adelson, and S. Levine, "More than a feeling: Learning to grasp and regrasp using vision and touch," *IEEE Robotics and Automation Letters*, vol. 2, no. 4, pp. 3300–3307, 2018.

[24] M. T. Ciocarlie and P. K. Allen, "Hand posture subspaces for dexterous robotic grasping," *The International Journal of Robotics Research*, vol. 28, no. 7, pp. 851–867, 2009.

[25] R. S. Fearing and J. M. Hollerbach, "Basic solid mechanics for tactile sensing," *The International journal of robotics research*, vol. 4, no. 3, pp. 40–54, 1985.

[26] M. R. Cutkosky, R. D. Howe, and W. R. Provancher, "Force and tactile sensors," in *Springer Handbook of Robotics*. Springer, 2008, pp. 455–476.